



LSTM-Based Deep Learning Methods for Prediction of Earthquakes Using Ionospheric Data

Rayan ABRI* , Harun ARTUNER 

Hacettepe University, Department of Computer Engineering, Ankara, Turkey

Highlights

- The paper focuses on earthquake prediction processes using ionospheric day by day variabilities.
- Due to the data capabilities, LSTM models are proposed for earthquake prediction.
- Highly precise accuracy was obtained to perform earthquake prediction.

Article Info

Received: 10 June 2021
Accepted: 10 Jan 2022

Keywords

Ionosphere
Total electron content
Lstm
Deep neural networks

Abstract

The ionosphere may play an essential role in the atmosphere and earth. Solar flares due to coronal mass ejection, seismic movements, and geomagnetic activity cause deviations in the ionosphere. The main parameter for investigating the structure of the ionosphere is Total Electron Content (TEC). TEC values obtained from GPS stations are a powerful technique for analyzing the ionospheric response to earthquakes and solar storms. This article analyzes the relations between earthquakes and TEC data to detect earthquakes. Our goal is to propose a prediction model to detect earthquakes in previous days. The ionospheric variability during moderate and severe earthquake events of varying strengths for 2012-2019 is discussed in this paper. The proposed models use LSTM-based (Long Short-Term Memory) deep learning models to classify earthquake days by analyzing TEC values of the last days. The LSTM-Based prediction models are compared against the SVM (Support Vector Machine), LDA (Linear Discriminant Analysis) classifier and Random Forest classifier to evaluate the proposed models based on earthquake prediction. The results reveal that the proposed models improve in detecting the earthquakes at an accuracy rate of about 0.82 and can be used as a successful tool for detecting earthquakes based on the previous days.

1. INTRODUCTION

As we gradually rise above the ground, we will encounter an atmospheric classification in terms of elevation, some of which will be of particular importance. The nature of molecules or ions that depend on the Earth's gravitational field changes the absorption of solar radiation and, therefore, temperature, density, and ionization. The boundaries of spatial layers are not constant, neither spatially nor temporally, because their interfering parameters are not fixed either. When moving away from the Earth's atmosphere, it reaches a layer from 48km to 965km (600mi) that is ionized to a plasma phase called the ionosphere layer.

A major measurable parameter that indicates a characteristic of the ionosphere is Total Electron Content (TEC). TEC provides an effective means to probe the structure of the ionosphere. In the literature, TEC is defined as the line integral of electron density along a ray path or as a measure of the total electrons along a ray path. The unit of TEC is given in TECU (TEC Unit), where TECU unit is equal to 10^{16} electron/ m^2 defined by Arikan et al. and Nayir et al. [1,2]. The fluctuations and turbulences of the ionosphere layer can be captured adequately and efficiently by calculating and watching TEC Values. Over the past few decades, the Global Positioning System (GPS) provides a cost-effective explication in calculating and assessing TEC

and observing the ionospheric layer turbulence over a notable proportion of global landmass as conducted by Nayir et al. [2].

Overall, the ionosphere layer's temporal and spatial variability directly relates to the earth's daily (each day) and annual rotation and the pattern of magnetic field lines of the geomagnetic dipole. As discussed by Rishbeth et al. [3], earth's magnetic field even when no existence of geomagnetic activities is scarcely quiet. The standard intermittent alterations generate the dynamics of the quiet ionosphere. The ionosphere's quiet conditions are impacted by the variations in the geomagnetic and solar activity and seismicity. So, these consequences can cause disturbances in parameters like earthquakes.

Empirically, discovering precursory signals in strong earthquakes is the subject of most case studies on earthquake prediction in the literature. Nevertheless, the precursory signals through long time periods are not investigated. This article proposes models to analyze the relationship between earthquakes and the ionospheric TEC data. The foremost aim of the recommended LSTM models is predicting an earthquake by analyzing previous days of the earthquake using ionospheric TEC data.

The rest of the article is prepared as follows. Section 2 discusses the related works on Total Electron Content fluctuation caused by geomagnetic and seismic disturbances in the ionosphere layer. Section 3 presents the ionospheric dataset and preprocessing phases for the processed models. We present our LSTM-based prediction models for the ionospheric data unified in Section 4. Evaluation methodology and results are discussed in Section 5 and 6, respectively. Section 7 includes the concluding remarks and future works.

2. RELATED WORK

This section presents the related works for monitoring the ionospheric disturbances expresses that geomagnetic activity like storms and earthquakes can cause intense disorders in the electron density distribution and TEC. The satellite-based measurements from GPS stations have implemented a useful study to investigate the seismo-ionospheric anomalies as described by Pulinets, and Tao et al. [4-7]. Biqiang and Trigunait et al. [8,9] investigated the ionospheric perturbation that storms can cause strong turbulence in the ionosphere's TEC values. Furthermore, Pulinets et al. [4] reported earthquakes and seismic activity could cause the changes in electromagnetic signals and the chemical composition of the atmosphere in the lithosphere with the troposphere and ionosphere.

Plenty of research like conducted works in [10-13] focus on statistical analyses about the experimental relationship between the ionospheric based irregularities and earthquakes. For example, the authors in [10] investigated statistically the TEC related to 20 strong (Magnitude \geq 6.0) earthquakes in Taiwan during the four years (1999–2002). They find out abnormalities that indicate the TEC value decreased within five days before the earthquakes through the other quiet days. Besides, Le et al. [11] illustrates the relation between ionospheric TEC based irregularities and strong earthquakes (Magnitude \geq 6.0) during nine years (2002–2010). Moreover, they confirmed a high rate of abnormalities happens in the ionosphere through earthquakes with Magnitude \geq 7.0 and depth \leq 20 km.

Recently Ulukavak, Pundhir, and Oikonomou et al. [2,14,15] have reported abnormal fluctuations in the ionospheric layer based on TEC values in the last days and several hours before severe or strong earthquakes. The TEC data has gathered from a GPS station in the earthquake zone. There are some uncertainty issues about generating such anomalies at the epicenter of the strong earthquakes. Tariq et al. [16], and Shah et al. [17] also stated direct relations between the ionosphere diversity and the existence of earthquakes. Their research demonstrated TEC values collected from the GPS receiver fluctuated and increased before Magnitude \geq 6.0 earthquakes occurred during the long term of 1998–2014. As referred by authors in [11], severe or intense earthquakes according to their magnitudes were listed based on the ionospheric TEC irregularities.

Suggested approaches in the literature based on earthquake prediction can divide into two principal sections [18]. The first is model-based approaches that hypothesize a machine learning model or a statistical model

to connected the earthquakes with seismic activities. The second is precursor-based approaches that focus on consideration of variations in the earthquake precursors.

Various machine learning approaches are used on past earthquakes to detect upcoming seismic activity based on seismic waveforms. These models are used in random forest, k-nearest neighbors, support vector machines (SVM), and artificial networks. (Asencio-Cortés et al. [19]; Mahmoudi et al. [20]; Moustra et al. [21]), In this research, we are focus on the most powerful Recurrent Neural Networks approaches such as LSTM-models to perform prediction on quiet and earthquake days.

Some research depends on the measurement of variations in the earthquake precursors using the ionosphere layer fluctuations called precursor-based methods [22,23]. Some other precursor-based methods use various factors instead of the ionosphere layer, such as strange lights, unknown animal action, the chemical construction of underground water, radon gas emissions, and temperature [24,25].

There is additionally various research that support anomaly detection approaches based on the ionospheric disturbances in ion temperatures, foF2, and TEC had been examined prior to severe earthquake nearby some country [26-28]. These studies based on machine learning and statistical models have been applied to impact seismic movements on the ionospheric layer irregularities, such as variation analysis and TEC difference or correlation investigation among TEC and foF2 or various combinations of GPS receivers. The authors in [29] aim to perform objective research on the precursor detection of a TEC-based earthquake. The study reported similarity among ionospheric TEC irregularities and severe earthquakes using threshold TEC anomaly signals.

As mentioned, the machine learning algorithms are performed on ionospheric data to extract the relationship between earthquakes and them [30,31]. The research [32] was conducted to review the correlation between earthquakes and ionospheric magnetic field disturbances that supervised machine learning methods are used to identify active seismic areas from the magnetic field in the ionosphere. The model is based on Random Forest and K-Means to detect potential relationships among magnetic disturbances in the ionosphere and seismic movements. Another research related to earthquake precursor detection [33] applies correlation methods to identify the influence of severe earthquake movement on the ionosphere layer. The study aims to detect anomalies connected with geomagnetic storms and earthquakes that correlate with GPS stations. However, the method can be executed for severe earthquakes.

The research, based on genetic algorithms, is applied [34], to detect earthquake precursors, and another study [35], has been used Artificial Neural Network to detect earthquake precursors by TEC data. The reason of using machine learning techniques to detect earthquake precursors is to consider the TEC data of the learning pattern. In some scenarios utilizing machine learning, an irregularity on TEC data may happen before the earthquake. Applying machine learning techniques based on N-Model Artificial Neural Network for detecting earthquake precursors has been made in Indonesia, particularly Sumatera [31]. The authors in [36] present a novel system that is called QuakeCast that detect short-term earthquake using global ionosphere TEC data. The proposed method using a classical logistic regression model and deep learning ConvLSTM autoencoder investigates whether signals foretell earthquakes in a TEC dataset of the ionosphere layer.

Following the conducted research in this field, we aim to analyze the prior days of the earthquakes using TEC values in the ionosphere layer and then classify the quiet and earthquake days in the target station zone. The main goal of this research is predicting the upcoming earthquakes in the prior days.

3. DATASET AND DATA PREPARATION

This section has introduced the dataset related to earthquakes and TEC values of GPS stations. The dataset preprocessing steps are also discussed in the following.

3.1. Dataset

As mentioned in Section 2, TEC values obtained from GPS stations are a powerful technique for analyzing the ionospheric response to earthquakes and solar storms. TEC data gathered from GPS stations (Dual-Frequency GPS receiver) is used to investigate the ionospheric variability through moderate and severe earthquakes. For this research, TEC data has been collected from two GPS stations. This data has been collected from the IONOLAB group (Hacettepe University of IONOLAB is an organization of electrical engineers to investigate hurdles of the ionosphere.)¹. The first station is located in coordinate (Lat: -20.15, Lon: -70.13) Iquique in Chile represented in Figure 1. The second station is located in coordinate (Lat: -20.85, Lon:117.1) Karratha in the Pilbara region of Western Australia represented in Figure 1. The earthquake information is collected via (United States Geological Survey of Earthquakes)².

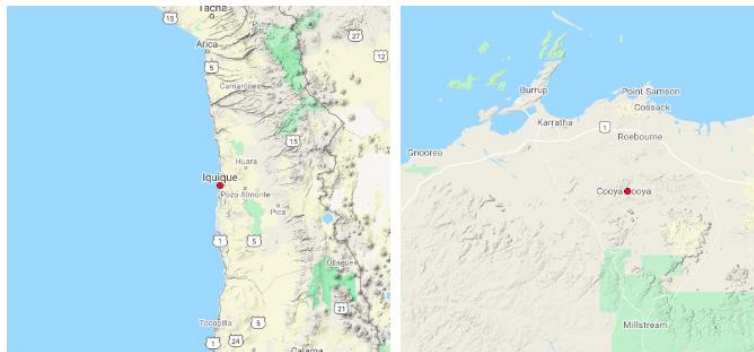


Figure 1. The Iqqe station is located in Coordinate (Lat: -20.15, Lon: -70.13) Iquique in Chile and the karr station located in coordinate (Lat: -20.85, Lon:117.1) Karratha in the Pilbara region of Western Australia

The ionospheric variability during moderate and severe earthquake events of varying strengths for 2012-2019 years is discussed in this paper. The data related to each station has been collected from 2012 to 2019. The data were separated day by day with 2880 TEC samples in a day. As illustrated in Figure 2, the stations are located in the same latitude from the two hemispheres of the east and west of the earth. The Chile region has strong and severe earthquakes; however, the Karratha region is almost quiet in terms of earthquakes.



Figure 2. Iqqe and Karr stations are located in the same latitude from the two hemispheres of the east and west of the earth

3.2. Data Preparation

In the machine learning concepts, the quality of the input dataset is so critical because there is a direct relationship between the quality of the input data and the performance of the trained model. Preprocessing of data consists of data tuning techniques that modify raw input data to an acceptable format. Ionospheric TEC data is often incomplete, inconsistent, and it is possible to contain many errors. Data preprocessing of this research consists of three phases, including Cleaning, Transformation, and Reduction.

¹ Available at <http://ionolab.org/>

² Available at <http://earthquake.usgs.gov/>

Since raw TEC data on specific days have missing and noisy values, the cleaning step attempts to eliminate missing values and make regressions with prior and later samples to smooth noisy values. Besides, the collected data is transformed into appropriate forms of mining. To perform the normalization, TEC values are scaled to a small, specified range (0-1.0). TEC data consists of 2800 samples in a day. In data mining, learning large amounts of input data that include many attributes leads to impractical or impossible analysis, and the training phase may take long times. Data Reduction includes practical techniques to reduce the dataset's input samples without hazarding the original data's integrity. The dataset is sampled TEC values every 15 minutes, and the data of a single day is reduced from 2800 to 95. It is evaluated the accuracy of the proposed model for the splitting of the train and test sets. Figure 3 demonstrate the accuracy in different train-test ratio. It is selected five different train-test ratios based on similar works in the literature. The different train-test ratio has been tested in the proposed single LSTM cell model. As depicted in the figure based on the accuracy, 80-20 ratio is a reasonable preference for the train-test ratio.

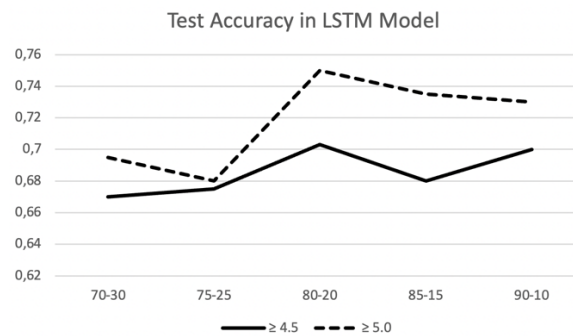


Figure 3. Performance metrics of the LSTM models in different train-test ratio based on two datasets (EQs ≥ 4.5 and EQs ≥ 5.0)

Table 1 illustrates some information about the ionospheric and the EQs(earthquakes) datasets. The table shows the collected data as details such as the ratio of the train and test sets.

Table 1. Prepared data for experimentation

Dataset Properties	Value
Number of days in uncleaned Dataset	2922
Number of days in cleaned Dataset	2571
Train-Test Ratio	80%-20%
Total number of earthquakes	79
Number of EQs ≥ 4.5 in Testset	16
Number of EQs ≥ 5.0 in Testset	10

The early studies have mentioned the ionosphere is affected by solar flares and other cosmic event factors. During the solar flares, X-ray fluxes are intensified that are identified as the cause of heightened ionization in the ionosphere. As this study focuses on ionospheric changes and the TEC variations during different earthquakes, it is needed to reduce the effect of solar flares and other cosmic events to recognize more correct earthquakes or geomagnetic activities.

As mentioned before, the stations are located at the same latitude from the two hemispheres of the east and west of the earth. Since the solar flares and other similar cosmic events affect the two hemispheres of the east and west of the earth, it can be calculated the similarity between two stations. The anomalies in the same days between the stations demonstrate the solar flares and other similar cosmic events. It can be assumed that they have the same abnormalities due to the solar flares and the other cosmic events in the corresponding stations. It is required to calculate the similarity between the stations to decrease the effect of these anomalies.

For this purpose, it is estimated the similarity between coincided days in each station in the dataset. Because of the nature of the dataset, it is considered cosine similarity to estimate the similarity between coincided days in each station. Cosine similarity is a metric between two non-zero vectors and is characterized by the cosine of the angles among the vectors. The cosine similarity is calculated as Equation (1)

$$\cos(x, y) = \frac{x \cdot y}{\|x\| \|y\|} = \frac{\sum_{i=1}^n x_i y_i}{\sqrt{\sum_{i=1}^n x_i^2} \sqrt{\sum_{i=1}^n y_i^2}} \quad (1)$$

where x and y are the vectors of the TEC data related to each day in the stations.

The dataset is used in the proposed LSTM models is balanced. That means a fixed ratio exists between the number of going to be predicted quiet days and the number of predicted earthquake days. As depicted in the structure dataset in Figure 4, samples in the prediction process have eight continuous days that will predict the 8th day's event of an earthquake or quiet day with examining the previous seven days. Every row in the dataset has eight continuous days, and each day has 94 ionospheric TEC samples and a cosine similarity field.

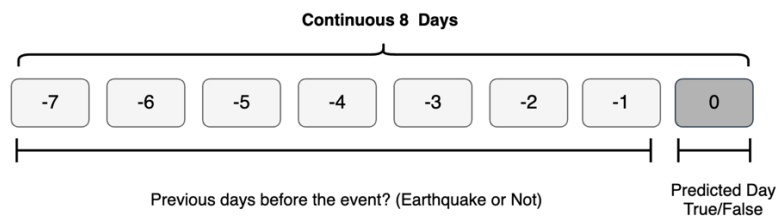


Figure 4. Dataset structure used in the proposed LSTM based models

4. METHODOLOGY OF SEQUENTIAL LEARNING

In this section, the architecture of the proposed model is presented. Due to the large amount of the TEC data related to each station, it is used deep neural networks. As the TEC data fluctuations in prior days of the earthquakes play a critical role in the prediction phase, it is planned to implement a sequential learning approach. In the literature, the analysis of learning algorithms for sequential data is sequential learning. In our sequential learning approach, the sequential dependency between TEC data is analyzed at the algorithmic level.

The sequence learning approaches are most generally based on sliding window methods and recurrent sliding windows. Sliding window-based methods disregard the relationship between data points inside the windows. However, model-based approaches, like the Markov chain defined on the data points that suppose sequential dependency between consecutive data.

4.1. LSTM-based Sequential Learning Models

Recurrent Neural Network (RNN) is a non-probabilistic model in which nodes satisfy the Markov-Chain assumption. An RNN network predicts the output label given the sequence of the TEC data from the past. One of the more accurate variants of the RNN methods is Long Short-Term Memory Networks (LSTM) that learn long term dependencies in sequence data. Due to the TEC data sequence related to previous days being long enough, RNN's may leave out critical information from the beginning. The LSTM methods handle this issue with the solution to short-term memory. These methods can adjust the flow of information with internal mechanisms called gates.

Figure 5 demonstrates the typical structure of the LSTM neural network cells is configured mainly by gates. Input gate takes a new input TEC data, memory in $(t-1)$ time step takes feedback from the LSTM cell's output in the last iteration. Deciding when to forget the output results is the task of the forget gate.

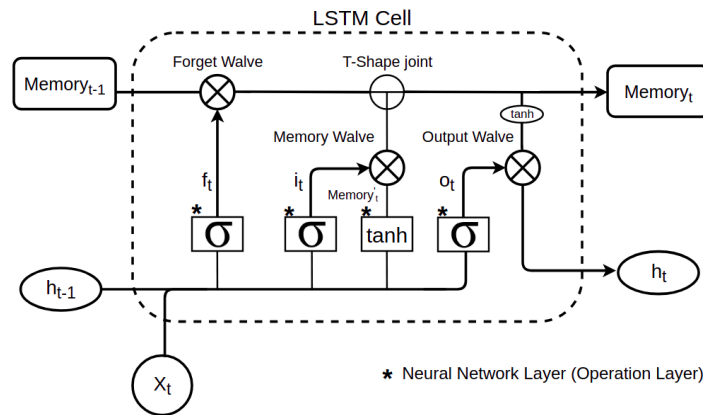


Figure 5. Structure of LSTM neural network cell

As illustrated in the LSTM cell formula in Equation (2), $X = (x_1, x_2, \dots, x_7)$ represents our TEC data separated by days. The proposed LSTM model is planned to use the previous seven days of the earthquakes and quiet days to perform prediction. The hidden state of memory cells is calculated in the Equation (2)

$$\begin{aligned}
 i_t &= \sigma(x_t U^i + h_{t-1} W^i) \\
 f_t &= \sigma(x_t U^f + h_{t-1} W^f) \\
 o_t &= \sigma(x_t U^o + h_{t-1} W^o) \\
 Memory'_t &= \tanh(x_t U^g + h_{t-1} W^g) \\
 Memory_t &= \sigma(f_t * Memory_{t-1} + i_t * Memory'_t) \\
 h_t &= \tanh(Memory_t * o_t)
 \end{aligned}
 \tag{2}$$

where i, f, o respectively represent the input gate, forget gate, and the output gates. g describes the candidate's internal state. W and U are the weight matrix and recurrent connections between the prior hidden and current hidden layers. The $Memory'$ is a candidate hidden state memory based on the current input and prior hidden state. $Memory$ is a combination of the prior memory multiplied by the forget gate. σ stands for the standard sigmoid function defined in Equation (3)

$$\sigma(x) = \frac{1}{1 + e^x}
 \tag{3}$$

The variant versions of the LSTM models are used to enhance the contribution of this research. For this purpose, deep-bidirectional LSTM [37] and Stacked LSTM [38] are evaluated. In the Bi-LSTM model, two LSTMs are applied to the input data. The Bi-LSTM consists of two operation layers. The first is the forward layer that applied an LSTM on the input data, and the second is the reverse mode of the input data fed into the LSTM model called the backward layer. Stacked LSTMs were introduced by Pascanu, et al. [38] for solving complex sequence prediction problems.

The stacked LSTM structure presents in Figure 6. The Stacked LSTM model fed on TEC sequence input data that some critical memory is kept for further use. The model stacks another dense layer that uses the earthquake labels of input data to perform prediction based on classification.

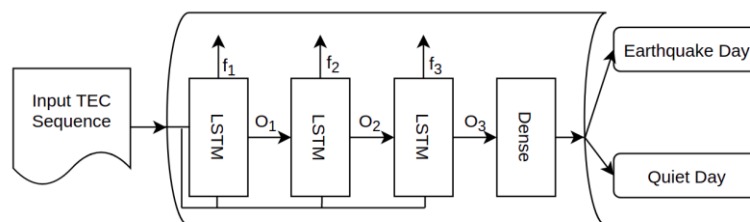


Figure 6. Structure of Stacked LSTM

The hyper parametric of the proposed LSTM models is represented in the Table 2, As stated in the table, it used hyperbolic tangent in the proposed LSTM models as activation functions. Adam is an optimizer that has been composed predominantly for deep neural networks algorithms. Adam optimizer estimates learning rates for various parameters as known as an adaptive learning rate approach. It is used estimations moments of the gradient to adaptively optimize the learning rate for every weight of the deep neural network. The detail of the training parameters is mentioned in the table. The training set is divided into training and validation set to find out the point of overfitting using the validation and training errors. The epoch size is fixed to 2000, however, the training of the network is stopped in 1823 epochs due to the validation and training error being crossed.

Table 2. The hyperparameters of the proposed system

Property	Proposed Models
Activation Function	hyperbolic tangent
Optimizer	Adam
Loss Function	BinaryCrossentropy
Dropout	0.25
Epoch size	2000/Stopped in 1823
Batch size	32
Decay Rate	0.97
Learning Rate	Adaptively optimize

5. EVALUATION METHODOLOGY

This section discusses learning parameters and evaluation metrics used for evaluation and helps better understand the metrics required to do a quality evaluation.

As mentioned in Section 4; finally, the TEC values separated by days are classified with the proposed models in the method section. Model evaluation metrics are required to measure the performance of a model. The choice of evaluation metrics depends on the model. As to the nature of data and proposed model, we use the accuracy, precision and recall as performance metrics. Here accuracy is a common evaluation metric for classification models. It is defined as the number of correct predicted earthquakes to the ratio of all classified days made. Precision is the ratio of correctly predicted earthquake days to the total classified days as earthquake days. The recall is the measure of our model correctly identifying earthquake days to the total of earthquake days. Depending on the data and specifications of the classification model, it is needed to emphasize precision or recall. The nature of this research is the classification of ionosphere disturbances based on the earthquakes to perform prediction. The ionospheric disturbances may cause events other than earthquakes. Therefore, in the prediction model, the count of false positives may be tolerable.

In generic classification models, between precision and recall values exist an association or trade-off. F1-score implies a measure of a test set efficiency that reflects both the precision and the recall to compute the score. The F1-score is the harmonious average of precision and recall in Equation (4)

$$F_1 - score = 2 * \frac{precision*recall}{precision+recall} \quad (4)$$

The splitting of the dataset to train and test set is used to predict the performance of machine learning algorithms. As mentioned in Table 1, it is apportioned the dataset into train and test sets, with an 80-20 split ratio. In the dataset, there is no proper proportion between the number of quiet days and the number of earthquake days. Therefore, there are only 79 earthquakes (Magnitude \geq 4.5) between 2012 to 2019. In the prediction model, we have a small number of earthquake classes. The Dataset has a small number of earthquake classes, which causes a problem called the unbalanced classification in the model. The class imbalance problem occurs when a class is comparatively rare as compared with other classes. Many methods have been proposed for imbalanced classification by Lopez-Paz, and Makki et al. [39,40], and

some good results have been reported. For solving the unbalanced dataset, we used the same count of quiet days and earthquake days.

K-fold cross-validation has been applied to improve the trustworthiness of the classification models based on prediction. The k-fold cross-validation uses the repeated random sampling technique to evaluate model's performance by dividing the data into $n=10$ equal folds and assessing the performance of the model on each fold. For analysis of the days, a ten-fold cross-validation plan is used for testing.

To examine the importance of the proposed LSTM based models, we used the SVM (Support Vector Machine) classifier to perform prediction based on finding a hyperplane in an N-dimensional space. The most trustworthy hyperplane means the one with the largest margin between the quiet days and earthquake days. As the issue of the earthquake classification is based on the prediction using the time series TEC data, SVM can be expanded efficiently to the task of regression and time series prediction. It is out of the scope of this paper to illustrate the theory on SVM thoroughly. SVM is a learning machine that indicates that a linear function ($f(x) = wx + b$) is consistently utilized to solve the regression problem. The most reasonable line is determined to be that line that minimizes the cost function in Equation (5)

$$Cost = \frac{1}{2} |w|^2 + K \sum_{i=1}^N L^\varepsilon(x_i + y_i + f) \quad (5)$$

where the L^ε is the loss function for each of the N training points. K is a positive constant that specifies the amount up to which deviations from ε are tolerated.

To For more contribution, it has been used various classifiers to perform prediction such as LDA (Linear Discriminant Analysis) based on the reduction of the features as conducted work by authors [41] and Random forest classifiers. Random Forest algorithm contains a considerable number of particular decision trees of TEC data group related to the days that operate cooperatively. Each tree in the random forest spits out a class prediction. Linear discriminant analysis is performed utilizing a max function M being a classification rule base prediction

$$f_i(X) = \frac{1}{(2\pi)^{\frac{1}{2}} |\Sigma|^{\frac{1}{2}}} \exp \left[-\frac{1}{2} (X - \mu_i)^T \Sigma^{-1} (X - \mu_i) \right] \quad (6)$$

$$M(X) = X^T \Sigma^{-1} \mu_i - \frac{1}{2} \mu_i^T \Sigma^{-1} \mu_i + \log(p_i). \quad (7)$$

The conditional density of X in class i is $f_i(X)$, p_i is the probability of class i. It is supposed that the vector of features X is variable and it is distributed with mean vector μ_i and common covariance matrix Σ . Next, $f_i(X)$ can be calculated as demonstrated in Equation (6). $M(X)$ discriminant function is computed as Equation (7) using the Bayes rule.

6. EVALUATION RESULTS

Using the evaluation methodology defined in Section 5, performances of our proposed LSTM models, the SVM, LDA and Random Forest classifiers are evaluated in terms of earthquake prediction. This section is organized to compare and examine the performance metrics of the classification models.

Table 2. Comparison of the proposed LSTM models and other classification models to perform prediction using performance metrics

Model	Accuracy	Precision	Recall	F1-score
LSTM EQs \geq 4.5	0.703	0.672	0.793	0.728
Bi-LSTM EQs \geq 4.5	0.720	0.697	0.787	0.739
Stacked- LSTM EQs \geq 4.5	0.787	0.777	0.812	0.794
SVM EQs \geq 4.5	0.659	0.640	0.756	0.693

LDA EQs \geq 4.5	0.604	0.590	0.656	0.621
Random Forest EQs \geq 4.5	0.640	0.619	0.731	0.670
LSTM EQs \geq 5.0	0.750	0.726	0.820	0.770
Bi-LSTM EQs \geq 5.0	0.740	0.701	0.840	0.7647
Stacked- LSTM EQs \geq 5.0	0.806	0.768	0.881	0.821
SVM EQs \geq 5.0	0.673	0.672	0.755	0.705
LDA EQs \geq 5.0	0.640	0.628	0.691	0.657
Random Forest EQs \geq 5.0	0.670	0.653	0.750	0.692

Table 2 describes the percentage of performance metrics like accuracy, recall, precision, and F1-score for the proposed LSTM based prediction models and the SVM, LDA and Random Forest prediction models based on two datasets. The first six rows illustrate the comparison between the proposed models and the other prediction models based on all earthquakes with a dataset that is magnetite \geq 4.5. It is evident that the proposed model has higher performance in all metrics than the SVM and other prediction models. The Stacked LSTM model boosted its precision and recall much more than the other prediction models. The ionosphere layer disturbances reflect all cosmic and seismic activities. As the false positive count is high in some scenarios in the dataset, precision is lower than recall and accuracy. The last six rows compare the LSTM prediction models and the SVM, LDA and Random Forest prediction models based on more strong earthquakes (magnetite-EQs \geq 5.0). Since the strong earthquakes affect the ionosphere more than moderate earthquakes, they are classified efficiently.

Figure 7 is the bar chart of performance metrics between the models in terms of two datasets (EQs \geq 4.5 and EQs \geq 5.0). It can be seen that in Figure 6 (Accuracy), the accuracy of the LSTM based grows slightly in the two mentioned datasets. Precision is a measure of prediction result relevancy based on earthquakes and false alarms, while recall is a measure of the classifier's ability to find and predict all the earthquake days. The comparison between datasets shows that the LSTM based models are more stable than the SVM and other prediction models in performance. Overall, Figure 5 reveals the Stacked-LSTM approach notably increases the precision, recall, and F1-score. Consequently, the improved performance in the dataset EQs \geq 4.5 is more extensive than the dataset EQs \geq 5.0, and the LSTM based models are more reliable in all earthquakes.

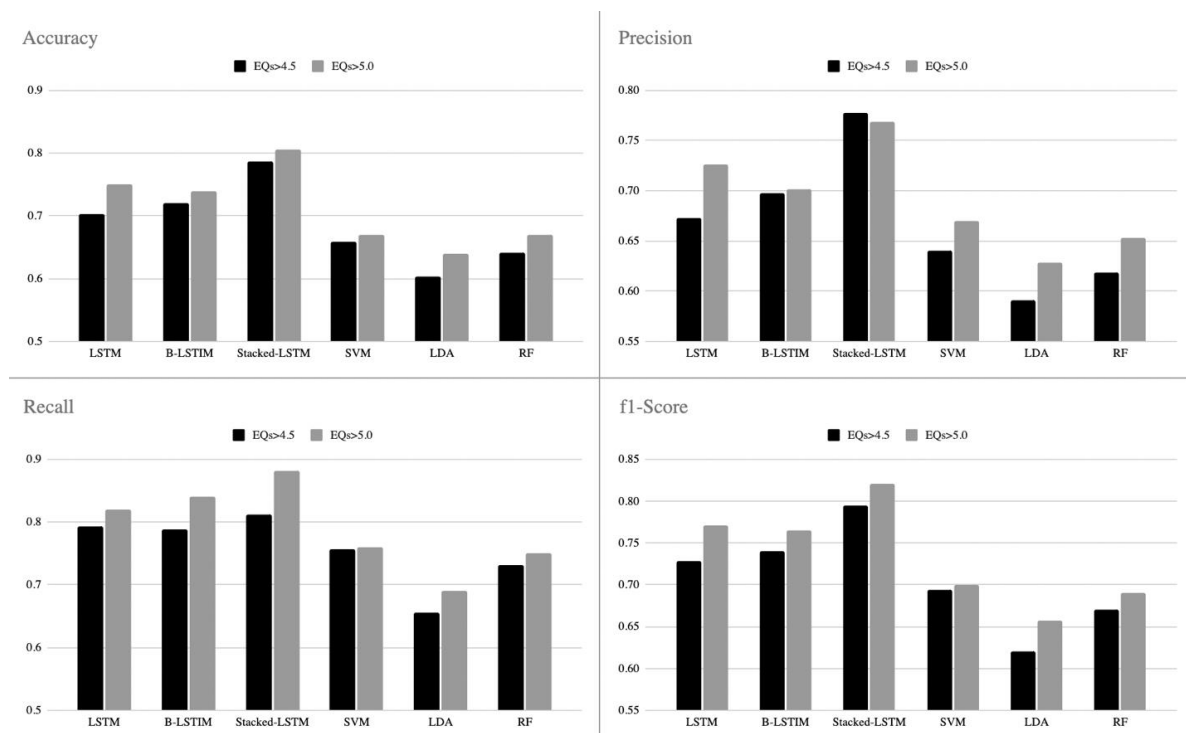


Figure 7. Performance metrics of the LSTM models and other prediction models based on two datasets (EQs \geq 4.5 and EQs \geq 5.0)

It can be beneficial to summarize each classifier's performance into a single measure to compare different prediction models. Receiver Operating Characteristic (ROC) curve is a common and standard measure with calculating the area under the curve to compare different prediction models. The ROC curve depicted the relation between the true-positive rate and the false-positive rate.

Classifiers that give curves closer to the top-left corner indicate a more trustworthy performance. As shown in the results, SVM is more accurate than Random Forest and LDA prediction models. So In the ROC table, we compare proposed LSTM models and SVM prediction model. Figure 8 depicts the ROC curve of the LSTM based models and the SVM prediction model based on two datasets. ROC curves related to the Stacked-LSTM positioned progressively closer to the upper left angle in ROC space, So the Stacked-LSTM has the progressively more prominent discriminant capacity of earthquake prediction. As depicted in the figure, the LSTM based models, and the SVM visually be compared simultaneously, and the results show the LSTM based models are more efficient than the SVM prediction model.

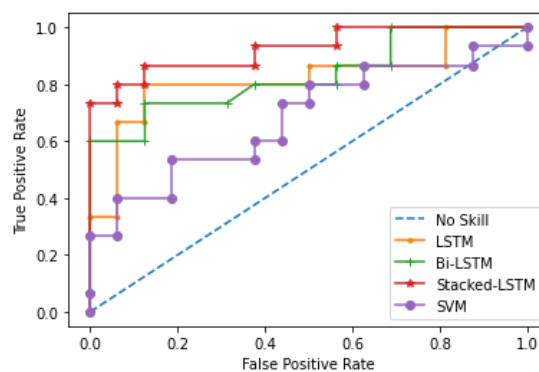


Figure 8. ROC curve of the LSTM based models and the SVM prediction model

AUC (Area Under the Curve) is an effective and combined measure of the true-positive and the false-positive rates for evaluating the intrinsic efficacy of the prediction models. The larger AUC means diagnostic tests are perfect in differentiating earthquake days from quiet days. The results in Table 3 demonstrates AUC values of the models for each dataset. The value of AUC in the Stacked-LSTM is 0.92, while in the SVM model is 0.60, which means a keen improvement in the ROC metric.

Table 3. AUC values for the LSTM models and the SVM

Model	ROC AUC
LSTM	0.821
Bi-LSTM	0.831
Stacked- LSTM	0.925
SVM	0.603

For further inspection of the proposed model, a statistical test is used to search for the level of significance and improvement. The null hypothesis assumes no distinction between the detected earthquake days and quiet days in the test. The p-value test is performed to decide whether the null hypothesis being tested can be rejected or not. The P-Value is the possibility of observing the effect(E) when the null hypothesis is true. In the test result of the Stacked-LSTM, the difference in performance over all metrics is significant ($p\text{-value} \ll 0.01$).

7. CONCLUSION

This research proposes an approach to detect earthquakes based on ionospheric TEC values. We proposed predictive models to predict ionosphere disturbances based on earthquakes using earlier days of earthquakes using LSTM based deep learning models. Ionospheric TEC data has been collected from two GPS stations. The Chile region has strong and severe earthquakes; however, the Karratha region is almost quiet in terms of earthquakes.

The principal intention of this research is to attain the relationship between earthquakes and the ionosphere disturbances based on deep learning techniques concerning LSTM based prediction models. To investigate the contribution of the recommended LSTM models, we used the SVM, LDA and Random Forest classifiers to perform earthquake prediction. Our results indicate approximately 80-85 accuracy-based performance in the two test sets of the earthquakes, including moderate and severe earthquakes. The proposed Stacked-LSTM has a more trustworthy and reliable performance than the SVM in terms of accuracy, recall, precision, F1-score, and ROC curve metrics.

ACKNOWLEDGMENT

This study is supported by IONOLAB group in Turkey. All Space Weather services provided in the IONOLAB website are developed using TUBITAK grants. These services are for academic and research purposes only. This article is a thesis article and produced from the Ph.D. thesis [42].

CONFLICTS OF INTEREST

No conflict of interest was declared by the authors.

REFERENCES

- [1] Arikan, F., Erol, C., Arikan, O., "Regularized estimation of vertical total electron content from global positioning system data", *Journal of Geophysical Research Space Physics*, A12, (2003).
- [2] Nayir, H., Arikan, F., Arikan, O., Erol, C., "Total electron content estimation with Reg-Est", *Journal of Geophysical Research Space Physics*, A11, (2007).
- [3] Rishbeth, H., Garriott, K., "Introduction to ionospheric physics", New York Academic Press, 14: 345-379, (1969).
- [4] Pulinets, S., Ouzounov, D., Karelin, A., Davi-denko, D., "Lithosphere atmosphere ionosphere magnetosphere coupling a concept for pre-earthquake signals generation", *Pre-Earthquake Processes: A Multidisciplinary Approach to Earthquake Prediction Studies*, 3: 79-99, (2018).
- [5] Pulinets, S., Contreras, L., Bisiacchi-Giraldi, G., Ciralo, L., "Total electron content variations in the ionosphere before the Colima, Mexico, earthquake of 21 January 2003", *Geofisica Internacional*, 4: 369-377, (2005).
- [6] Tao, D., Jinbin, C., Battiston, R., Li, L., Yudian, M., Wenlong, L., Wang, L., Dunlop, W., "Seismo-ionospheric anomalies in ionospheric TEC and plasma density before the 17 July 2006 M7. 7 south of Java earthquake", *Annales Geophysicae*, 35(3): 589-598, (2017).
- [7] Arslan, T., Munawar, M., Pajares, H., Iqbal, T., "Pre-earthquake ionospheric anomalies before three major earthquakes by GPS-TEC and GIM-TEC data during 2015-2017", *Advances in Space Research*, 7: 2088-2099, (2019).
- [8] Biqiang, Z., Weixing, W., Libo, L., Tian, M., "Morphology in the total electron content under geomagnetic disturbed conditions: results from global ionosphere maps", *Annales Geophysicae*, 7: 1555-1568, (2007).
- [9] Trigunait, A., Parrot, M., Pulinets, S., Feng, L., "Variations of the ionospheric electron density during the Bhuj seismic event", *Annales Geophysicae*, 12: 4123-4131, (2004).
- [10] Liu, J., Chen, Y., Chuo, J., Chen, C., "A statistical investigation of pre-earthquake ionospheric anomaly", *Journal of Geophysical Research Space Physics*, A5, (2006).

- [11] Lopez-Paz, D., Sra, S., Smola, A., Ghahramani, Z., Scholkopf, B., “Randomized nonlinear component analysis”, *International Conference on Machine Learning*, 10: 1359-1367, (2014).
- [12] Oikonomou, C., Haralambous, H., Muslim, B., “Investigation of ionospheric TEC precursors related to the M7. 8 Nepal and M8. 3 Chile earthquakes in 2015 based on spectral and statistical analysis”, *Natural Hazards*, 11: 97-116, (2016).
- [13] Pundhir, D., Singh, B., Kumar, S., Gupta, S., Pathak, K., “Study of ionospheric precursors using GPS and GIM-TEC data related to earthquakes occurred on 16 April and 24 September 2013 in the Pakistan region”, *Advances in Space Research*, 9: 1978-1987, (2017).
- [14] Huijun, L., Liu, J., Liu, L., “A statistical analysis of ionospheric anomalies before 736 M6. 0+ earthquakes during 2002–2010”, *Journal of Geophysical Research Space Physics*, 3: 87-102, (2011).
- [15] Enlu, L., Chen, Q., Xiaoming, Q., “Deep reinforcement learning for imbalanced classification”, *Applied Intelligence*, 21: 1-15, (2020).
- [16] Liu, J., Chuo, Y., Shan, S., Tsai, Y., Chen, I., Pulnits, A., Yu, S., “Pre-earthquake ionospheric anomalies registered by continuous GPS TEC measurements”, *Annales Geophysicae*, 22(5): 1585-1593, (2004).
- [17] Liu, J., Chen, C., Chen, Y., Yang, W., Oyama, I., Kuo, W., “A statistical study of ionospheric earthquake precursors monitored by using equatorial ionization anomaly of GPS TEC in Taiwan during 2001–2007”, *Journal of Asian Earth Sciences*, 2: 76-80, (2010).
- [18] Bendick, R., Bilham, R., “Do weak global stresses synchronize earthquakes?”, *Geophysical Research Letters*, 44(16): 8320-8327, (2017).
- [19] Asencio-Cortes, G., “Improving earthquake prediction with principal component analysis: application to Chile”, *International Conference on Hybrid Artificial Intelligence Systems*, 3: 393-404, (2015).
- [20] Mahmoudi, J., Arjomand, M., Rezaei, M., Mohammadi, M., “Predicting the earthquake magnitude using the multilayer perceptron neural network with two hidden layers”, *Civil Engineering Journal*, 2(1): 1-12, (2016).
- [21] Moustra, M., Avraamides, M., Christodoulou, C., “Artificial neural networks for earthquake prediction using time series magnitude data or seismic electric signals”, *Expert Systems with Applications*, 38(12): 15032-15039, (2011).
- [22] Gulyaeva, L., Arikani, F., Stanislawski, I., “Persistent long-term (1944–2015) ionosphere-magnetosphere associations at the area of intense seismic activity and beyond”, *Advances in Space Research*, 59(4): 1033-1040, (2017).
- [23] Oyama, K., Devi, M., Kwangsun Ryu, C., Chen, C., Liu, J., Bankov, L., Kodama, T., “Modifications of the ionosphere prior to large earthquakes: report from the ionosphere precursor study group”, *Geoscience Letters*, 3(1): 1-10, (2016).
- [24] Fidani, C., “The earthquake lights (EQL) of the 6 April 2009 Aquila earthquake, in Central Italy”, *Natural Hazards and Earth System Sciences*, 10(5): 967-978, (2010).
- [25] Grant, A., Halliday, T., “Predicting the unpredictable; evidence of pre-seismic anticipatory behaviour in the common toad”, *Journal of Zoology*, 281(4): 263-271, (2010).

- [26] Akhoondzadeh, M., “Decision Tree, bagging and random forest methods detect TEC seismo-ionospheric anomalies around the time of Chile, (Mw= 8.8) earthquake of 27 February 2010”, *Advances in Space Research*, 57(12): 2464-2469, (2016).
- [27] Davidenko, V., Pulinets, S., “Deterministic variability of the ionosphere on the eve of strong ($M \geq 6$) earthquakes in the regions of Greece and Italy according to long-term measurements data”, *Geomagnetism and Aeronomy*, 59(4): 493-508, (2019).
- [28] Li, W., Jinyun, G., Jianping, Y., Yang, Y., Zhen, L., Deikai, L., “Contrastive research of ionospheric precursor anomalies between Calbuco volcanic eruption on April 23 and Nepal earthquake on April 25, 2015”, *Advances in Space Research*, 57(10): 2141-2153, (2016).
- [29] Akyol, A., Arikan, O., Arikan, F., Deviren, M., “Investigation on the reliability of earthquake prediction based on ionospheric electron content variation”, *16th International Conference on Information Fusion*, 1658-1663, (2013).
- [30] Arikan, O., Arikan, F., Akyol, A., “Machine learning based detection of earthquake precursors using ionospheric data”, *42nd COSPAR Scientific Assembly*, 42, (2018).
- [31] Aji, B., Houw, L., Buldan, M., “Detection precursor of sumatra earthquake based on ionospheric total electron content anomalies using N-Model artificial neural network”, *International Conference on Advanced Computer Science and Information Systems (ICACSIS)*, 269-276, (2017).
- [32] Nowakowski, A., Chris, S., Lorenzo, T., Floberghagen, R., Kilbane-Dawe, I., “A machine learning approach to investigate possible signals in the ionosphere related to earthquake activity”, *Geophysical Research Abstracts*, 21, (2019).
- [33] Muslim, B., “Examination of correlation technique for detecting the influence of great earthquake activities on Ionosphere”, *Jurnal Sains Dirgantara*, 12(2): (2015).
- [34] Akhoondzadeh, M., “Genetic algorithm for TEC seismo-ionospheric anomalies detection around the time of the Solomon (Mw= 8.0) earthquake of 06 February 2013”, *Advances in Space Research*, 52(4): 581-590, (2013).
- [35] Akhoondzadeh, M., “Investigation of GPS-TEC measurements using ANN method indicating seismo-ionospheric anomalies around the time of the Chile (Mw= 8.2) earthquake of 01 April 2014”, *Advances in Space Research*, 54(9): 1768-1772, (2014).
- [36] Reid, J., Jeffrey, L., Bhavani, A., “QuakeCast, an earthquake forecasting system using ionospheric anomalies and machine learning”, *AGU Fall Meeting Abstracts*, NH007-0016, (2020).
- [37] Schuster, M., Paliwal, K., “Bidirectional recurrent neural networks”, *IEEE Transactions on Signal Processing*, 45(11): 2673-2681, (1997).
- [38] Pascanu, R., Gulcehre C., Kyunghyun, C., Bengio, Y., “How to construct deep recurrent neural networks”, *ArXiv Preprint ArXiv:1312.6026*, (2013).
- [39] Munawar, S., Shuanggen, J., “Statistical characteristics of seismo-ionospheric GPS TEC disturbances prior to global $Mw \geq 5.0$ earthquakes (1998–2014)”, *Journal of Geodynamics*, 5: 42-49, (2015).
- [40] Sharma, A., Paliwal, K., “Linear discriminant analysis for the small sample size problem: an overview”, *International Journal of Machine Learning and Cybernetics*, 3: 443-454, (2015).

- [41] Tharwat, A., Gaber, T., Ibrahim, A., Hassanien, A., “Linear discriminant analysis: A detailed tutorial”, *AI Communications*, 30(2): 169-190, (2017).
- [42] Abri, R., "Modeling of the ionosphere's disturbance using deep learning techniques", PhD. Thesis, Hacettepe University, Graduate School of Science and Engineering, Ankara, (2021).